ELSEVIER

International Journal of Mass Spectrometry 204 (2001) 185–196

International Journal of Mass Spectrometry

Dissociation mechanisms for metal N-glycosides of N-acetyl neuraminic acid

Michael D. Leavell, Julie A. Leary*

Department of Chemistry, University of California, Berkeley, CA 94720, USA

Received 10 November 1999; accepted 26 May 2000

Abstract

Metal(II) N-glycoside complexes of N-acetyl neuraminic acid are synthesized and analyzed by electrospray ionization ion trap mass spectrometry. The dissociation products for various ligands (1,3-diaminopropane and diethylenetriamine) and metals (Co, Ni, Cu, Zn) are compared and contrasted. Most notable were the differences in the cross-ring cleavages: the ^{0,4}X cross-ring cleavage seems to be favored by the 1,3-diaminopropane ligand, whereas the ^{0,2}X, ^{0,4}X–H_2O, and ^{0,4}X cross-ring cleavages are prevalent in the diethylenetriamine ligand complexes. Dissociation mechanisms are postulated based on the results of ^{2}H and ^{13}C labeling experiments. (Int J Mass Spectrom 204 (2001) 185–196) © 2001 Elsevier Science B.V.

Keywords: Transition metal; Monosaccharide; Electrospray ionization; Quadrupole ion trap; Mass spectrometry

1. Introduction

As the field of glycobiology grows, so does the need for more suitable analytical techniques that can be used to elucidate the structure of carbohydrates. Complete structure elucidation requires the determination of stereochemistry (e.g. D-galactose versus D-mannose), anomericity (α versus β) and linkage between monomers. Currently no single analytical technique allows for complete carbohydrate structural elucidation.

Mass spectrometry is becoming a more commonly used technique for elucidation of carbohydrate structure [1–10]. The advantages of mass spectrometry include the speed with which analyses are performed and its low sample consumption [1]. Furthermore, tandem mass spectrometry allows for the identification of the components of a heterogeneous mixture, thus requiring less sample purification.

In our laboratory, structural characterization of carbohydrates is achieved through metal or metal/ligand complexation followed by tandem mass spectrometry [5,11–21]. Stereochemical differentiation of the metal–ligand systems has been tested with promising results using the biologically relevant hexoses [11], hexosamines [14] and N-acetyl-hexosamines [15]; however, other monosaccharides are still under investigation. In the studies presented herein, N-acetyl neuraminic acid was chosen to study the effects of our metal–ligand systems on the dissociation of more complex monosaccharides.

Sialic acids normally occur as terminal components of oligosaccharides [22]. N-acetyl neuraminic acid is nine-carbon carboxylated monomer (Fig. 1) which is the precursor of all other sialic acids [23].

* Corresponding author. E-mail: leary@socrates.berkeley.edu.

PII S1387-3806(00)00365-1

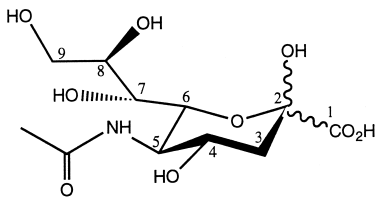

Fig. 1. N-acetyl-α-D-neuraminic acid (carbons are labeled).

The biological roles of these compounds are very diverse. Although many functions are still under scrutiny, a commonly recognized role of sialic acids is to mediate intercellular interaction. A well-known example is found in the inflammatory process [24]. White blood cell adhesion to activated endothelial cells occurs through interaction of sialyl-Lewis^x with E-selectin. It is this interaction that localizes the immune response to infected areas of the body. Other biological roles of sialic acid include protection from the binding of pathogenic viruses [23], and as markers for the onset of oncogenesis [22].

Given the important role of the sialic acids in biological systems, characterization is paramount. Therefore, this study is aimed at the analysis and investigation of possible dissociation mechanisms of Neu5Ac complexed with different ligands and metals, so that in subsequent analysis of larger oligomers, characteristic dissociation patterns of the various sialylated complexes will be easily recognized. The ligands, 1,3-diaminopropane and diethylenetriamine, have two or three coordinating nitrogens, respectively. Thus, different coordination environments can be investigated for each metal. Four different transition metal centers are employed with each ligand: Co(II), Ni(II), Cu(II), and Zn(II), allowing for the evaluation of different electronic effects. Each complex is analyzed by tandem mass spectrometry and product ions are verified through isotopic labeling experiments.

Influence on the dissociation mechanisms is seen from the variation of the ligands and the metals. When comparing the cross-ring cleavages, the most notable differences depend on the identity of the ligand. For example, the ^{0,4}X cross-ring cleavage seems to be favored by the 1,3-diaminopropane ligand (dap), whereas the ^{0,2}X, ^{0,4}X–H_2O, and ^{0,4}X cross-ring cleavages are favored by the diethylenetriamine (dien) ligand. The prevalence of different cross ring cleavages for different metal centers are interpreted based on possible coordination of the metal centers. For example, when the dap ligand is employed the Co(II) and the Ni(II) metal ions, which are normally six coordinate, have unfilled coordination spheres [16–18]. This unsaturation in the coordination sphere appears to promote the ^{0,4}X cross-ring cleavage, however, the ^{0,2}X and the ^{0,4}X–H_2O cross-ring cleavages are absent. Upon ring opening, it is the fulfillment of the Co(II) and the Ni(II) coordination spheres that causes the ^{0,2}X cross-ring cleavage to become disfavored. However, when Zn(II) a normally four-coordinate metal center is utilized, both cross-ring cleavage mechanisms are favored.

2. Experimental

2.1. Instrumentation

All experiments were performed on the Finnigan LCQ quadrupole ion trap mass spectrometer (Finnigan MAT, San Jose, CA), fitted with an electrospray ionization (ESI) source. Samples were infused using a syringe pump at a rate of 2 μL/min. Ionization was achieved using a spray voltage of 5.0 kV. In order to keep space charge effects to a minimum, the automatic gain control was set at 5×10^7 counts for MS^1 experiments, while a value of 2×10^7 counts was employed for all MS^n experiments. These values are the default settings for the LCQ instrument. The maximum ion inject time was set at 100 ms. Ion guide voltages were tuned to maximize the precursor ion current using the auto-tune feature of the LCQ.

The tandem mass spectrometry (MS/MS) isolation width of the precursor ion was selected to include its full isotopic distribution. Collision-induced dissociation (CID) was performed at a q value of 0.25 by applying a supplementary voltage across the endcaps for 30 ms. The voltage was applied at the axial secular frequency of the precursor ion and with an amplitude of 0.68, 0.71, 0.76, or 0.71 V for the $[M(dien)(Neu5Ac)–H]^+$ com-

plexes (where M = Co, Ni, Cu, and Zn, respectively, and Neu5Ac = N-acetyl neuraminic acid); whereas an amplitude of 0.65, 0.75, 0.70, or 0.73 V for the $[M(dap)(Neu5Ac)–H]^+$ complexes was utilized. Helium was used as the collision gas in all experiments, and was maintained at a pressure of 1 mTorr. Each spectrum is an average of 20 scans. A criterion of 3% relative abundance has been utilized to determine the absence or presence of product ions [5].

2.2. Synthesis: stock solutions

An 8.1 mM stock solution of Neu5Ac was prepared in 200 μL of 50:50 H_2O:methanol [high-performance liquid chromatography (HPLC) grade]. The 1-3-diaminopropane (6.0 mM), diethylenetriamine (55.0 mM) and metal chloride stock solutions [$CoCl_2 \cdot 6H_2O$ (16 mM), $NiCl_2 \cdot 6H_2O$ (11 mM), $CuCl_2 \cdot 2H_2O$ (36 mM) $ZnCl_2$ (26 mM)] were made in HPLC grade methanol.

A 1:1.1 mole ratio of Neu5Ac (80 nmol) and the appropriate ligand (1,3-diaminopropane or diethylenetriamine) were added to 200 μL of HPLC grade methanol to give a final concentration of 0.4 mM. The reaction mixture was refluxed in a borosilicate tube at 63 °C for 20 min, and diluted to 20 pmol/μL with methanol. Prior to analysis 1.5 equivalents of the metal salt (Co, Ni, Cu, Zn) was added to a portion of the diluted mixture and vortexed to facilitate complexation.

2.3. Labeling studies

The metal/N-glycoside complexes were synthesized as above. H/D exchange of the hydroxyl, amide, and carboxylic acid protons was accomplished by diluting the solutions in 200 μL CH_3OD prior to analysis. All deuterated samples were analyzed by ESI using perdeuterated solvents. [1-^{13}C] labeled metal/N-glycoside complexes were synthesized as above using N-acetyl-D-[1-^{13}C]neuraminic acid.

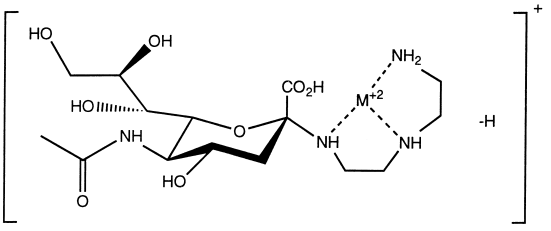

Fig. 2. $[Metal(II)/dien/Neu5Ac–H]^+$.

2.4. Chemicals and materials

N-acetyl neuraminic acid was obtained from Sigma Chemical Company (St. Louis, MO). 1-3-diaminopropane and diethylenetriamine were obtained from Aldrich Chemical Company (Milwaukee, WI). $ZnCl_2$, $NiCl_2 \cdot 6H_2O$, and $CoCl_2 \cdot 6H_2O$ were obtained from Fisher (Fairborn, NJ), and $CuCl_2 \cdot 2H_2O$ was purchased from Malinckrodt (Paris, KN). HPLC grade methanol and water were purchased from Sigma-Aldrich (Milwaukee, WI). N-acetyl-D-[1-^{13}C]neuraminic acid was obtained from Omicron Biochemicals (South Bend, IN), and deuterated methanol was obtained from Aldrich Chemical Company (Milwaukee, WI). All materials were used as received without further purification.

3. Results and discussion

A total of eight Neu5Ac metal–ligand complexes were investigated. The different complexes were generated by varying the ligand: either 1,3-diaminopropane (dap) or diethylenetriamine (dien), or by varying the metal: Co, Ni, Cu, or Zn. Upon reacting Neu5Ac with the selected ligand, the N-glycoside complexes were formed [25–27]. The reaction of the monosaccharide with the ligand is a typical hydrolysis in which the anomeric hydroxyl group is converted to the N-glycoside with subsequent loss of water. Prior to analysis, the metal was added to the solution of the N-glycoside product, forming the $[metal(II)/ligand/Neu5Ac]^{+2}$ complex. The $[metal(II)/ligand/Neu5Ac–H]^+$ complex [Fig. 2 and Fig. 3 for the dien and dap complexes, respectively] was mass selected and allowed

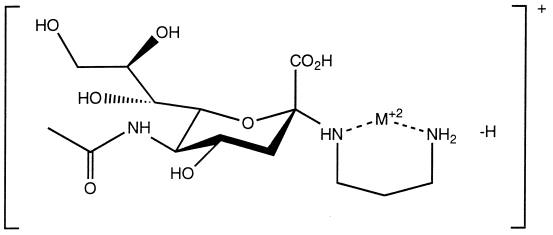

Fig. 3. [Metal(II)/dap/Neu5Ac–H]$^+$.

to undergo CID. The dissociation of these complexes (see Figs. 2 and 3) is discussed in the following.

One population of ions, consisting of a single ligand coordinated to a doubly charged metal ion is deprotonated in the gas phase. The site of deprotonation is unknown at this time, however labeling experiments discussed within, suggest specific locations. CID product ion spectra for the dien/Neu5Ac complexes with Co, Ni, Cu, and Zn are shown in Fig. 4(A)–(D), respectively. The commensurate dap/Neu5Ac CID spectra are provided in Fig. 5(A)–(D). Neutral losses from both the dien and the dap complexes are listed in Tables 1 and 2, respectively.

Three common features are observed in all dien spectra regardless of the metal center employed: loss of water (M–H_2O), loss of $C_4H_{10}O_5$ (^{0,4}X–H_2O), and loss of $C_8H_{15}O_6N$ (^{0,2}X) (Fig. 6) (^{m,n}X notation was developed by Domon and Costello [28]). The loss of 120 Da was observed for all metal/dien/Neu5Ac complexes. This loss is thought to originate from the ^{0,4}X cross-ring cleavage ($C_4H_8O_4$) for the Co, Ni, and Zn complexes. However, for the Cu complexes, it was

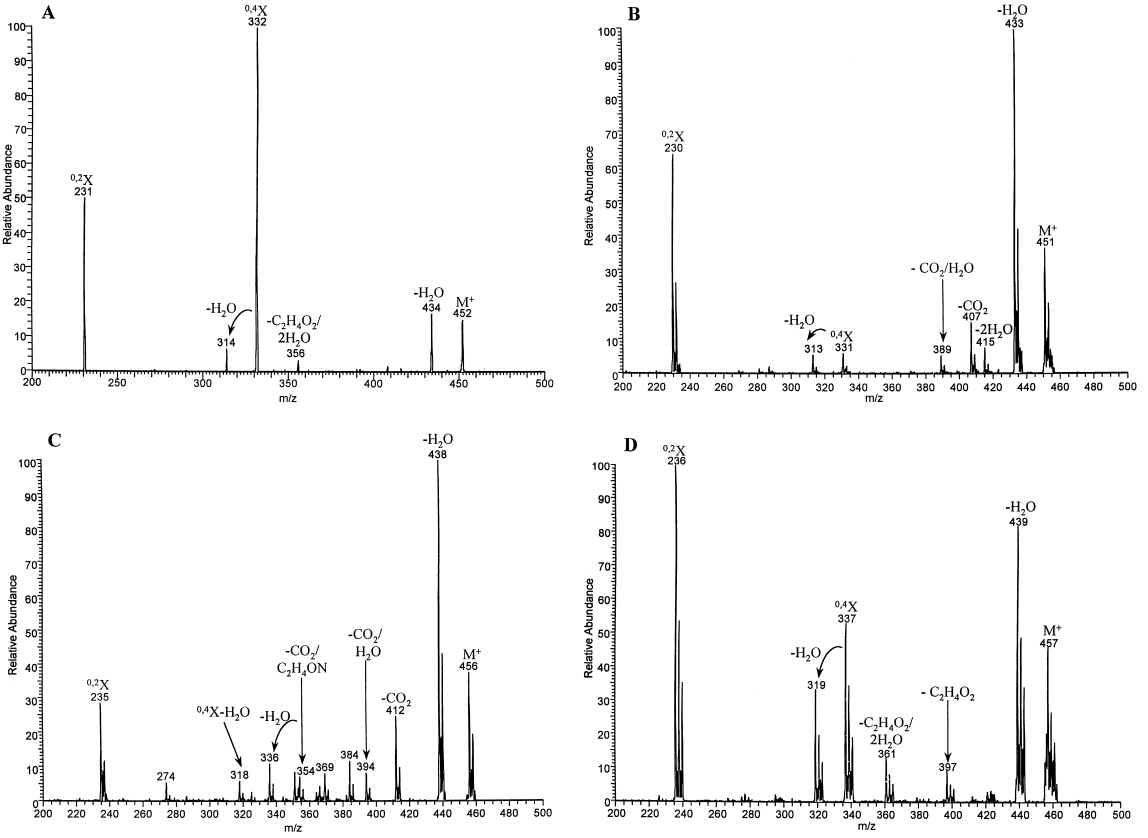

Fig. 4. Product ion spectra (MS^2) of the deprotonated metal (II) N-glycoside precursor ions: (A) [Co(II)/dien/Neu5Ac–H]$^+$ (*m/z* 452); (B) [Ni(II)/dien/Neu5Ac–H]$^+$ (*m/z* 451); (C) [Cu(II)/dien/Neu5Ac–H]$^+$ (*m/z* 456); and (D) [Zn(II)/dien/Neu5Ac–H]$^+$ (*m/z* 457).

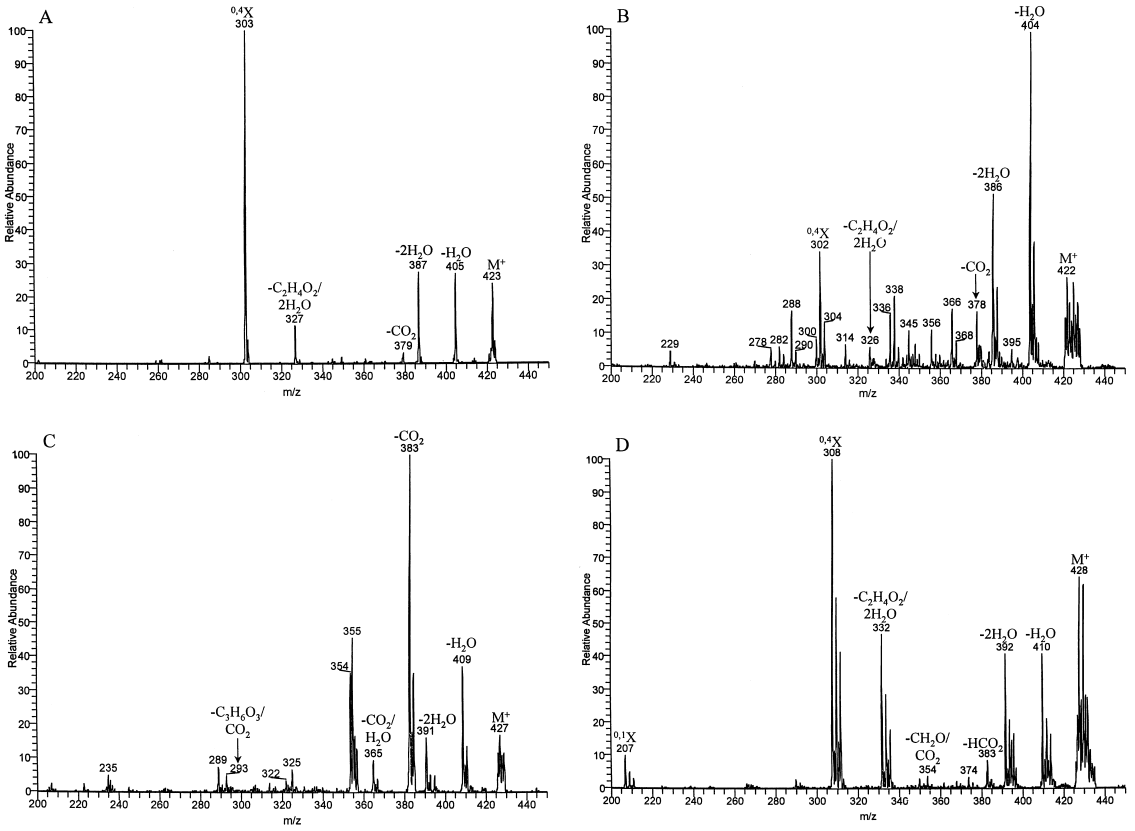

Fig. 5. Product ion spectra (MS^2) of the deprotonated metal (II) N-glycoside precursor ions: (A) $[Co(II)/dap/Neu5Ac–H]^+$ (*m/z* 423); (B) $[Ni(II)/dap/Neu5Ac–H]^+$ (*m/z* 422); (C) $[Cu(II)/dap/Neu5Ac–H]^+$ (*m/z* 427); and (D) $[Zn(II)/dap/Neu5Ac–H]^+$ (*m/z* 428).

determined through isotopic labeling experiments that a loss of C(1) occurred. This data is inconsistent with the ^{0,4}X cross-ring cleavage, and instead a radical mechanism [29–32] resulting in the loss of carbon dioxide, water, and the amide group is thought to occur.

One and two water molecules are the only common losses observed for the dap complexes. As in the dien complexes, loss of $C_4H_8O_4$ is found when the metal ions Co, Ni, and Zn are employed. However, the radical mechanism resulting in loss of 120 Da for the Cu complexes is not observed. Also, more strikingly, loss of $C_8H_{15}O_6N$ (^{0,2}X) is only observed for the Zn/dap complexes, whereas loss of $C_4H_{10}O_5$ (^{0,4}X–H_2O) is not observed at all.

Loss of CO_2 is prevalent in many of the postulated

Table 1
Selected $[metal(II)/dien/Neu5Ac–H]^+$ dissociations products[a]

	$-H_2O$	$-2H_2O$	$-CO_2$	$-C_2H_4O_2$	$-CO_2/H_2O$	$-C_2H_4O_2/2H_2O$	$-CO_2/C_2H_4ON$	$-CO_2/H_2O/C_2H_4ON$	$-C_4H_8O_4$	$-C_4H_{10}O_5$	$-C_8H_{15}O_6N$
Co	×					×			×	×	×
Ni	×	×	×		×				×	×	×
Cu	×		×		×		×	×		×	×
Zn	×			×		×			×	×	×

[a] An × indicates the presence of the dissociation product at an ion intensity of greater than 3% of the base peak.

Table 2
Selected [metal(II)/dap/Neu5Ac–H]$^+$ dissociation products[a]

	$-H_2O$	$-2H_2O$	$-CO_2$	$-HCO_2$	$-CO_2/H_2O$	$-CH_2O/CO_2$	$-C_2H_4O_2/2H_2O$	$-C_4H_8O_4$	$-C_3H_6O_3/CO_2$	$-C_4H_{10}O_5$	$-C_8H_{15}O_6N$
Co	×	×	×				×	×			
Ni	×	×	×				×	×			
Cu	×	×	×		×				×		
Zn	×	×		×		×	×	×			×

[a] An × indicates the presence of the dissociation product at an ion intensity of greater than 3% of the base peak.

dissociation mechanisms. Often, subsequent neutral losses from the [M–CO_2]$^+$ ion occurs, such as: loss of H_2O, CH_2O, or $C_3H_6O_3$. When dien is employed as a ligand, CID of the Ni, Cu, and Zn complexes only, show losses containing CO_2. However, when the dap ligand is employed, spectra generated from complexes with all different metals showed losses containing CO_2. The most likely source of these losses is the carboxylic acid functionality. Dissociations of metallated (Ni, Cu) amino acids also produce loss of CO_2 as product ions [29–32]. Similarly, they are postulated to originate from the carboxylate functionality. This data has been confirmed through ^{13}C labeling experiments as shown herein.

Several factors could influence the dissociation of the Neu5Ac complexes. Coordination geometry of the monosaccharide/ligand complex to the metal center has been shown to play a role in the types of dissociations being driven [13,16,17]. However, examination of product ion spectra does not yield any clear trends with regard to the metals employed. Another factor that could influence the dissociation of these complexes is the binding location of the metal.

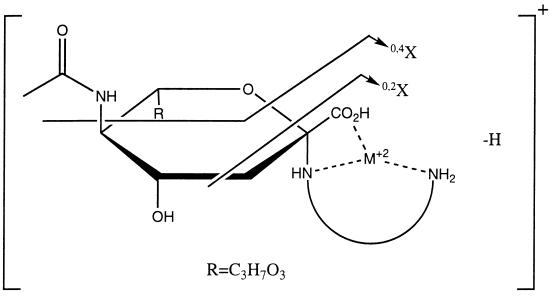

Fig. 6. Cross-ring cleavages of [metal(II)/ligand/Neu5Ac–H]$^+$ complexes.

A preference of binding between transition metals and nitrogen rather than oxygen has been documented by Martell and Calvin [33]. Brodbelt and co-worker, have observed preferential metal binding to pyridyl ligands over that of polyether ligands, in a study of ESI generated mixed ligand complexes [34,35]. Additionally, our group has shown through x-ray crystal structure analysis, that the metal ion is coordinated preferentially to the amine ligand [25]. Using these data, a likely binding site of the metal is postulated to be a binding pocket made up of the ligand and the carboxylic acid functionality. This is supported through analysis of CPK models, which illustrates this sterically favorable metal binding pocket and by the fact that the N-glycoside product of the hydrolysis reaction is specific to the anomeric carbon [26,27]. Therefore, the postulated metal binding location is specific, and product ions should all result from metal containment in the proposed binding pocket.

Another apparent factor influencing the cross-ring cleavages of the metal/ligand/Neu5Ac complexes is the coordination number of the metal. CID of the metal/dien/Neu5Ac complex promotes all cross-ring cleavages. In this case, three nitrogens are known to coordinate the metal ion [11–13]. However, CID of the metal/dap/Neu5Ac complex, in which only two nitrogens are available for coordination, results in only the $^{0,4}X$ cross-ring cleavage. Further implications of metal coordination are discussed in Sec. 3.1.

3.1. Labeling studies

Although logical neutral losses can be postulated a priori, a verification of the neutral losses through

Table 3
^{2}H labeled [Co(II)/dien/Neu5Ac–H]$^{+}$ dissociation products

	$-D_2O$	$-C_2H_2D_2O_2/2D_2O$	$-C_4H_5D_3O_4$	$-C_4H_5D_5O_5$	$-C_8H_{10}D_5O_6N$
Co	×	~	×	~	×

[a] An × indicates the presence of the dissociation product at an ion intensity of greater than 3% of the base peak and a tilde indicates the ion intensity was less than 3% of the base peak.

isotopic labeling studies strengthens the proposed dissociation mechanisms. Therefore, both ^{2}H and ^{13}C labeling studies were undertaken.

Deuterium labeling experiments were performed to determine the number of exchangeable protons contained in the product ions. The metal/dien/Neu5Ac complexes contain ten exchangeable protons, while the metal/dap/Neu5Ac complexes contain a total of nine exchangeable protons. Monoisotopic cobalt was utilized as the metal of choice in the deuterium labeling experiments. Both the Co/dap and the Co/dien complexes show the loss of $C_4H_5D_3O_4$. This is consistent with loss of the glycerol moiety through a $^{0,4}X$ cross-ring cleavage (Fig. 6; Tables 3 and 4). The $^{0,2}X$ cross-ring cleavage results from the loss of $C_8H_{10}D_5O_6N$ for the Co/dien complex. The $^{0,2}X$ cross-ring cleavage contains five exchangeable protons; these are consistent with loss of the glycerol moiety, the amide group, and the C(4) hydroxyl group. The nitrogen rule verifies the likely loss of the amide nitrogen in the $^{0,2}X$ cross-ring cleavage. Because of the very low relative abundance of the resulting product ions (<3%) [5] neither the loss of $C_2H_2D_2O_2/2D_2O$ nor $C_4H_5D_5O_6N$ could be verified. Ions corresponding to these losses were observed, however, their intensities were between 1% and 3%. In these cases the ions are designated by a tilde in the data tables.

Table 4
^{2}H labeled [Co(II)/dap/Neu5Ac–H]$^{+}$ dissociation products[a]

	$-D_2O$	$-2D_2O$	$-C_2H_2D_2O_2/2D_2O$	$-C_4H_5D_3O_4$
Co	×	×	~	×

[a] An × indicates the presence of the dissociation product at an ion intensity of greater than 3% of the base peak and a tilde indicates the ion intensity was less than 3% of the base peak.

Several product ions appeared to result from the loss of CO_2 from the carboxylic acid functionality. To determine if the loss of C(1) occurs, complexes labeled with ^{13}C at the C(1) position were allowed to undergo CID. The ^{13}C labeling data, which shows only those losses containing CO_2, are contained in Tables 5 and 6. The dien complexes (Table 5) indicate four losses, all of which contain $^{13}CO_2$. Similarly, CID of the dap complexes (Table 6) also showed that any losses of CO_2 incorporated the C(1) carbon. In some instances, the ions resulting from loss of $^{13}CO_2$ were below the criteria of 3% relative abundance [5] and in these cases the losses are again indicated by a tilde. Of particular interest is the fact that, as was the case with the nonlabeled CID data, there are differences in the presence and absence of CO_2 product ions depending on the metal ion and ligand used.

Interestingly, the ^{13}C labeling experiments highlighted a radical mechanism in which CO_2, H_2O and the amide functionality are lost. This loss is unique to the [Cu/dien/Neu5Ac–H]$^{+}$ complex. Originally the loss of 120 Da was assumed to result from the $^{0,4}X$ cross-ring cleavage. However, upon completion of the labeling study, the loss of 120 Da was found to include C(1).

Table 5
Dissociation products of [metal(II)/dien/Neu5Ac $^{13}C(1)$–H]$^{+}$ resulting from loss of $^{13}CO_2$[a]

	$-{}^{13}CO_2$	$-{}^{13}CO_2/H_2O$	$-{}^{13}CO_2/C_2H_4ON$	$-{}^{13}CO_2/H_2O\ C_2H_4ON$
Co				
Ni	×	×		
Cu	×	×	×	×
Zn				

[a] An × indicates the presence of the dissociation product at an ion intensity of greater than 3% of the base peak.

Table 6
Dissociation products of [metal(II)/dap/Neu5Ac $^{13}C(1)$–H]$^+$ resulting from loss of $^{13}CO_2$[a]

	$-{}^{13}CO_2$	$-H{}^{13}CO_2$	$-{}^{13}CO_2/H_2O$	$-CH_2O/{}^{13}CO_2$	$-C_3H_6O_3/{}^{13}CO_2$
Co	~				
Ni	×				
Cu	×		~		×
Zn		~		~	

[a] An × indicates the presence of the dissociation product at an ion intensity of greater than 3% of the base peak and a tilde indicates the ion intensity was less than 3% of the base peak.

3.2. Mechanisms: loss of $C_4H_8O_4$, $C_4H_8O_4$–H_2O, $C_8H_{15}O_6N$, and CO_2

Based on the ^2H and the ^{13}C labeling studies, mechanisms of dissociation are proposed and presented below. For clarity only the dissociation mechanisms from the cobalt complexes are discussed; the elemental compositions from the labeling experiments are listed in parenthesis.

One population of ions, consisting of a single ligand coordinated to a doubly charged metal ion, is deprotonated in the gas phase. The deprotonated dien complexes are likely tetradentate as evidenced previously [11–13,25] although the possibility of additional coordination from the glycerol moiety, or other available hydroxyl groups, can not be excluded at this time. Precedence has also been shown for three-coordinate dap complexes with Ni^{2+} [16–18] and again, although additional coordination can occur with the sialylated oligosaccharides, it is not unreasonable that some population of precursor ions may exist as the tricoordinate unsaturated complex. At this point there is no concrete scientific evidence that can unambiguously identify the coordination geometry about the metal ion. However, what is obvious from the data presented herein, is that the dissociation of these complexes are different and these differences are exacerbated by both the coordinating metal ion and the ligand, which has different numbers of nitrogen available for coordination.

One intriguing feature observed with these complexes (also observed extensively in previously reported studies of metal-coordinated oligosaccharides [12–18]) is the hypothesis that populations of ions exist that have different sites of deprotonation. Tangential to this is also the possibility that ground state ions are all deprotonated at the carboxyl group, but that upon activation, proton migration occurs which allows for different heteroatoms to be deprotonated thus giving rise to very specific product ions. The sources of many of these product ions are verified through the labeling studies. Thus the mechanisms proposed herein are based on the current information obtained from the specific labeling experiments. Determining whether the site of deprotonation giving rise to a specific labeled dissociation ion was initially deprotonated or subject to proton migration is beyond the scope of this paper.

The postulated mechanism for loss of $C_4H_8O_4$ ($C_4H_5D_3O_4$) begins with the deprotonation of the aminal nitrogen (**1**) (Scheme 1), whereby monosaccharide ring opening is initiated and the generation of a secondary alkoxide ion results (**2**). Although one would preferentially identify the carboxylic functionality as the site of deprotonation under normal solution conditions, coordination of a N or O to the metal center in the gas phase will easily force deprotonation of the heteroatom. This is likely if there are different populations of ions such that in some cases the carboxylate is coordinated to the metal, but in other cases it is not and a stronger chelation is affected through the hydroxyl or amino functionality. Given the results obtained from both the ^2H and ^{13}C labeling data, it is clear that there is more than one site of deprotonation on the molecule thus generating different populations of precursor ions. For example, in order to see loss of $C_4H_5D_3O_4$ (carbons 6, 7, 8, and 9), the site of deprotonation for this population of precursor ions must generate from the aminal and cause ring opening as shown in Scheme 1. Two possible dissociation pathways may follow. One such pathway (pathway 1) is the formation of a cyclobutane ring [21,36], allowing the loss of $C_4H_8O_4$ ($C_4H_5D_3O_4$) (**3**). Baldwin's rules for ring closure [37] add credence to the mechanism in spite of the steric strain of the product ion.

Another possible mechanism (pathway 2) involves carbanion formation through heterolytic cleavage of

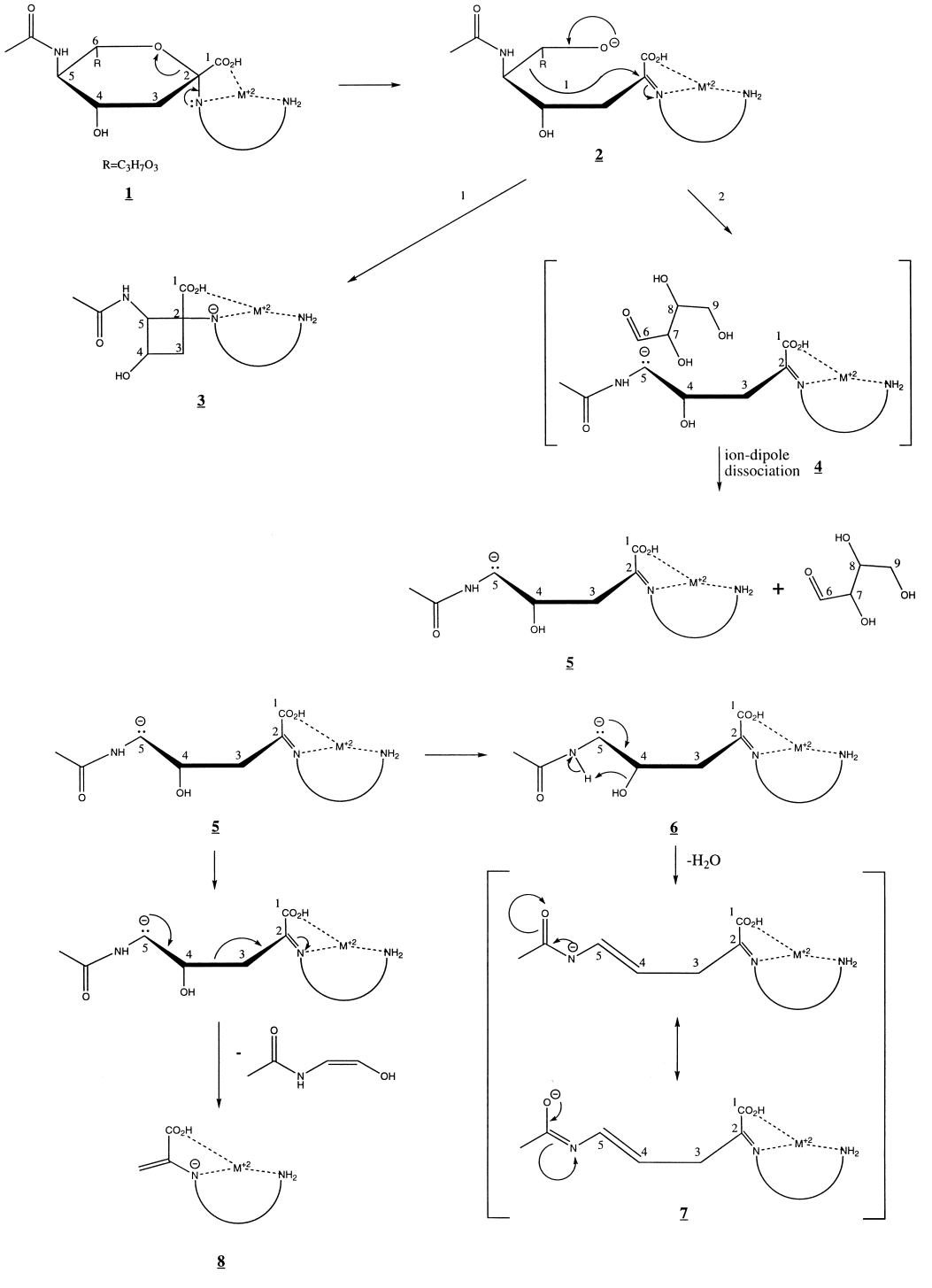

Scheme 1.

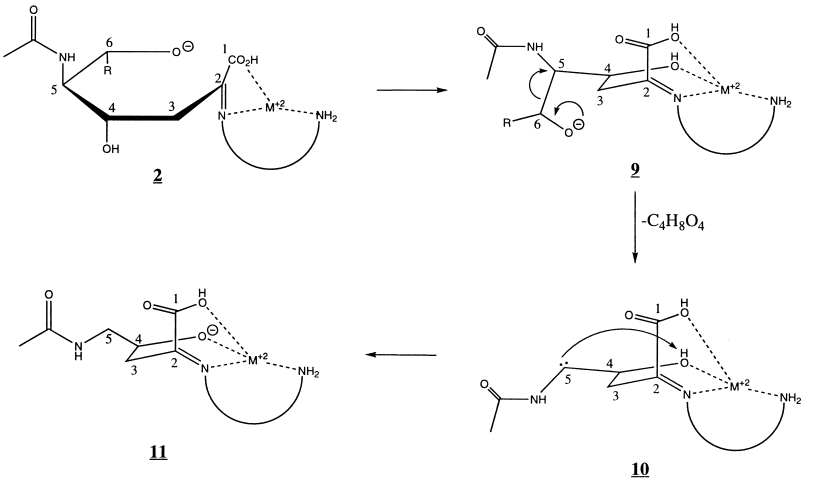

Scheme 2.

the C5–C6 sigma bond in which carbanion stabilization is achieved through an ion–dipole complex (**4**). Squires and co-worker [38] and Brauman and co-workers [39,40] have thoroughly documented the formation of such ion-dipole complexes in smaller systems. The obvious pathway from **4** is the dissociation of the ion–dipole complex to yield **5**.

Upon dissociation of the ion–dipole complex, stabilization of the free carbanion (**5**) is accomplished through intramolecular rearrangement generating complete losses of $C_4H_{10}O_5$ ($C_4H_5D_5O_5$) (**7**) and $C_8H_{15}O_6N$ ($C_8H_5D_5O_6N$) (**8**). Both losses result from a pathway where double bond formation occurs at C4–C5. This is initiated by electron donation to C4–C5 resulting in either transfer of the amide proton to the C4 hydroxyl group (**6**), producing loss of water (**7**), or continued dissociation through cleavage of C3–C4 resulting in **8**. Product ion (**7**) is resonance stabilized through the amide group.

Cross-ring cleavage mechanisms are postulated to be driven by the coordinatively unsaturated metals. This is illustrated by the fact that the Co(II) and the Ni(II) dap complexes only show the ^{0,4}X cross-ring cleavage. These metals possess partially filled d-shells and therefore favor coordination numbers of four or greater [41]. However only three coordination sites are available in the dap metal binding pocket (Scheme 2). Therefore upon ring opening (**9**) the unsaturated metal centers are postulated to coordinate to the C(4) hydroxyl group creating a four coordinate complex. Once this extra interaction has occurred both the ^{0,2}X and the ^{0,4}X–H_2O cross-ring cleavages would be higher in energy and therefore disfavored. Upon metal coordination to the hydroxyl group, carbanion stabilization could be achieved through deprotonation of the hydroxyl group (**10**) leading to alkoxide coordination (**11**). In the case of Zn(II) however, both cross-ring cleavages are observed. The Zn(II) metal

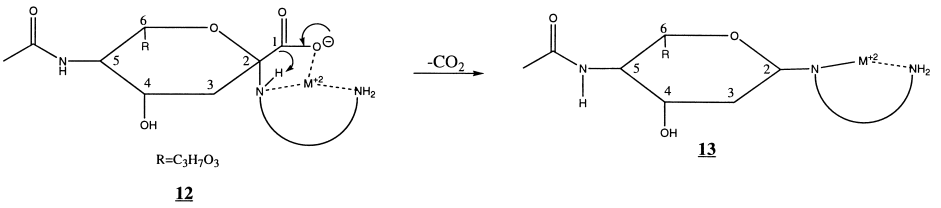

Scheme 3.

has a filled *d* shell, thus two- or three-coordinate complexes are stable and extra coordination is not required [41]. This difference drives the $^{0,2}X$ cross-ring cleavage in the case of Zn/dap complexes, while disfavoring the $^{0,2}X$ and the $^{0,4}X–H_2O$ cross-ring cleavages in the case of unsaturated metals.

Loss of CO_2 is believed to occur through deprotonation of the carboxylic acid (Scheme 3) (**12**). Upon CID decarboxylation occurs resulting in loss of CO_2 followed by a 1,2-H shift resulting in deprotonation of the aminal nitrogen (**13**). Stabilization of the nitrogen anion is achieved through coordination with the metal center.

4. Conclusions

Several features of deprotonated metal/N-glycoside complexes were varied to determine the effect of various ligands and metals on the dissociation of N-acetyl neuraminic acid. This work has demonstrated that the dissociation of N-acetyl neuraminic acid is directed by different metals and ligands. Specifically, ligands with two coordinating nitrogens (1,3-diamiopropane) promote one and two water losses in combination with all four metals employed in this study. Further, the $^{0,4}X$ cross-ring cleavage is favored by the Co, Ni, and Zn metals. However, the diethylenetriamine ligand with three coordinating nitrogens promotes three cross-ring cleavage mechanisms irrespective of the metal center, e.g. $^{0,4}X$, $^{0,4}X–H_2O$, and $^{0,2}X$. Patterns in cross-ring cleavage mechanisms suggest a coordinatively unsaturated metal can direct cross-ring cleavage through coordination with other functional groups during ring opening. This coordination creates an energetically more stable complex, disfavoring certain cross-ring cleavages. The above losses were verified through ^{2}H and ^{13}C labeling experiments. In addition, it was determined that a number of losses resulted from a initial loss of CO_2 from the carboxylic acid functionality. These were verified through ^{13}C labeling experiments of C(1). From these data, dissociation mechanisms are postulated.

Acknowledgement

The authors gratefully acknowledge the NIH for funding this research (grant no. GM-47356).

References

[1] H. Geyer, R. Geyer, Acta. Anat. 161 (1998) 18.
[2] V.N. Reinhold, B.B. Reinhold, C.E. Costello, Anal. Chem. 67 (1995) 1772.
[3] A.S. Weiskopf, P. Vouros, D.J. Harvey, Anal. Chem. 70 (1998) 4441.
[4] K. Tseng, J.L. Hedrick, C.B. Lebrilla, Anal. Chem. 71 (1999) 3747.
[5] S. Koenig, J.A. Leary, J. Am. Soc. Mass. Spectrom. 9 (1998) 1125.
[6] B.L. Gillece-Castro, A.L. Burlingame, Meth. Enzymol. 193 (1990) 689.
[7] H. Egge, J. Peter-Katalinic, Mass Spectrom. Rev. 6 (1987) 331.
[8] S.G. Penn, M.T. Cancilla, C.B. Lebrilla, Anal. Chem. 68 (1996) 2331.
[9] M.R. Asam, G.L. Glish, J. Am. Soc. Mass Spectrom. 8 (1997) 987.
[10] J. Lemoine, D. Fournet, D. Despeyroux, K.R. Jennings, R. Rosenberg, E.J. de Hoffmann, J. Am. Soc. Mass Spectrom. 4 (1993) 197.
[11] S.P. Gaucher, J.A. Leary, Anal. Chem. 70 (1998) 3009.
[12] S.P. Gaucher, J.A. Leary, J. Am. Soc. Mass Spectrom. 10 (1999) 269.
[13] S.P. Gaucher, J.A. Leary, Int. J. Mass Spectrom. 197 (2000) 139.
[14] H. Desaire, J.A. Leary, Anal. Chem. 71 (1999) 1997.
[15] H. Desaire, J.A. Leary, Anal. Chem. 71 (1999) 4142.
[16] G. Smith, A. Kaffashan, J.A. Leary, Int. J. Mass Spectrom. Ion Processes 182/183 (1999) 299.
[17] G. Smith, J.A. Leary, J. Am. Chem. Soc. 120 (1998) 13046.
[18] G. Smith, S.F. Pedersen, J.A. Leary, J. Org. Chem. 62 (1997) 2152.
[19] G.E. Hofmeister, Z. Zhou, J.A. Leary, J. Am. Chem. Soc. 113 (1991) 5964.
[20] E.M. Sible, S.P. Brimmer, J.A. Leary, J. Am. Soc. Mass Spectrom. 8 (1997) 32.
[21] A. Fura, J.A. Leary, Anal. Chem. 65 (1993) 2805.
[22] A. Rosenberg, Biology of the Sialic Acids, Plenum, New York, 1995, pp. 7–50.
[23] A. Varki, Glycobiology 2 (1992) 25.
[24] L.A. Lasky, Science 258 (1992) 964.
[25] S.P. Gaucher, S.F. Pedersen, J.A. Leary, J. Org. Chem. 64 (1999) 4012.
[26] S. Yano, Coord. Chem. Rev. 92 (1988) 113.
[27] S. Yano, M. Kato, H. Shioi, T. Takahashi, T. Tsubomura, K. Toriumo, T. Ito, M. Hidai, S. Yoshikawa, J. Chem. Soc. Dalton Trans. (1993) 1699.
[28] B. Domon, C.E. Costello, Glycoconjugate J. 5 (1988) 397.

[29] C.L. Gatlin, F. Turecek, T. Vaisar, J. Mass Spectrom. 30 (1995) 1065.
[30] C.L. Gatlin, F. Turecek, T. Vaisar, J. Mass Spectrom. 30 (1995) 1617.
[31] C.L. Gatlin, F. Turecek, T. Vaisar, J. Am. Chem. Soc. 117 (1995) 3637.
[32] T. Yalcin, J. Wang, D. Wen, A.G. Harrison, J. Am. Soc. Mass Spectrom. 8 (1997) 749.
[33] A.E. Martell, M. Calvin, Chemistry of the Metal Chelate Compounds, Prentice Hall, Englewood Cliffs, NJ, 1956.
[34] J. Shen, J. Brodbelt, J. Mass Spectrom. 34 (1999) 137.
[35] J. Shen, J. Brodbelt, J. Am. Soc. Mass Spectrom. 10 (1999) 126.
[36] A. Staempfli, Z. Zhou, J.A. Leary, J. Org. Chem. 57 (1994) 3590.
[37] J. March, Advanced Organic Chemistry: Reactions, Mechanisms and Structure, 3rd ed., Wiley, New York, 1985, p. 187.
[38] S.T. Graul, R.R. Squires, J. Am. Chem. Soc. 112 (1990) 2517.
[39] W. Tumas, R.F. Foster, M.J. Pellerite, J.I. Brauman, J. Am. Chem. Soc. 109 (1987) 961.
[40] W. Tumas, R.F. Foster, J.I. Brauman, J. Am. Chem. Soc. 110 (1988) 2714.
[41] F.A. Cotton, G. Wilkinson, Advanced Organic Chemistry, 5th ed., Wiley Interscience, New York, 1966, pp. 597–622, 724–775.